
**SYNTHESIS OF APATITIC NANOFERTILIZER FOR SUSTAINABILITY OF
NATURAL PHOSPHATE ROCK**

Nimbona Guillaume*, Yaya Mahamat Idriss and Ech-Chahad Abdellah

¹University Hassan I, Laboratory of Applied Chemistry and Environment, Faculty of Sciences and Technology, BP 577 Settat (Morocco)

ABSTRACT

In this study, we focused our interest on the synthesis of a porous nanofertilizer having an apatitic structure from a raw natural phosphate in alkaline medium. To obtain this nanofertilizer type, the natural phosphate rock initially enriched by sieving, was submitted to chemical extraction in presence of an alkaline salt as a digesting agent. The obtained apatite was treated with a cationic surfactant in order to improve the porosity of the final product. The results of analyzes obtained by combining X-ray diffraction technique, B.E.T. measurements and TFIR infrared spectroscopy clearly showed that the obtained product was a nanoporous apatite. The apatite obtained by this combined process would be an important intermediate for the manufacturing of other various products of phosphate derivatives. It should be noted that this process is very effective to remove the elements with an acidic valence such as silica, organic carbon, chromium VI and vanadium V. On the other hand, Titanium and Yttrium, which have amphoteric valences, remain with Apatite in amorphous form and are thus reactive. The elements with a basic valence are difficult to remove by this process (Mg, Sr, Ca, Cd, Zn, Cu, Ce). The metals belonging to the actinides group, in particular uranium, are removed at a rate of 40%

Keywords: Phosphate rock, Apatite, nano-porosity, Sieving, Uranium, alkaline extraction.

1. INTRODUCTION

The temporal and environmental sustainability of crude phosphate is the one that is based on its exploitation in a form close to its original apatitic structure, especially since it is a finite and non-renewable resource [1]. Nevertheless, phosphate fertilizers are rarely produced and used as an apatite source because of their low solubility [2]. Acidic dissolution is a usual technique which is used for the manufacturing of fertilizers, but it is associated with numerous problems related to the denaturation of the apatitic structure due to the total loss of calcium and partial loss of phosphorus in the form of phosphogypsum ($\text{CaSO}_4 \cdot 2\text{H}_2\text{O} + \text{Ca}(\text{H}_2\text{PO}_4)_2 \cdot 2\text{H}_2\text{O}$). In addition, it is known that the application of natural phosphates as fertilizers in agriculture is often hindered by the large particle size, which limits their mobility in the soil and thus prevents phosphates to reach the root zone to feed crops in a timely manner [3-4]. It is for this reason that the use of nanofertilizer was proposed in order to maximize the uptake of nutrients by the plants from soil [5]. However, the direct absorption of nanofertilizer by plant roots can only occur if the

nanoparticles size are very small than the pore diameter of plant cell walls, which is comprised between 5 and 20nm[6]. In recent years, there has been much interest in exploitation of using surfactant-based methods for the synthesis of nanomaterials such as nanofertilizers [7]. These surfactants play a key role in the controlling of the reactions, size and shape of particles [8-9]. By using a surfactant, it is possible to obtain a nano-apatite with a well-hierarchized porosity and a high specific area[10-11].The aim of this work is to synthesize a nano-porous apatite as fertilizer in presence of Cetrimonium bromide[C₁₆H₃₃N(CH₃)₃]Br⁻as a structuring agent, which can be assimilated by plants.

2. MATERIALS AND METHODS

2.1 Enrichment of raw material

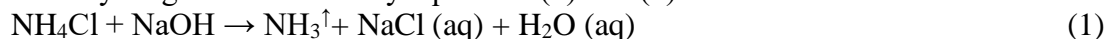
First, it should be noted that our raw rock phosphate ore was sampled in the region of Bengrir (Morocco). There are several techniques for the enrichment of phosphate ores, but in our study, we have used the sieving technique with two sieves having mesh openings 1000 and 90µm. In fact, the sieving is the simplest and most adequate technique for enriching a phosphate rock because it allows to make the particle size cut-off. This operation makes it possible to remove the particles of granulometries under 90 µm which are rich in silica, limestone, clay and fractions greater than 1000µm which are rich in sterile stones. Then, the oversize of this granulometric class was analyzed by X-ray diffraction in order to identify the phases associated with the apatite before its alkaline extraction (Fig.1a). The main functional groups of the raw phosphate rock was identified with an infrared spectroscopy technique (Fig.2).

2.2 Alkaline extraction with caustic soda

The enriched ore still contains some original impurities that is not possible to remove completely by traditional techniques. It is at this stage that the alkaline extraction process becomes effective for complete removal of amorphous silica and organic matter as well as some trace transition metals such as chromium and vanadium as well as some traces of transition metals such as chromium and vanadium. On the other hand, Titanium, Yttrium and Silver remain with Apatite. Some metals belonging to the lanthanide group such as Uranium, are eliminated at a rate of 40%. This fraction is bound to organic matter in complex form or as vanadate of uranyl and calcium. Indeed, these vanadates of uranyl and calcium have been identified in the calcareous or siliceous rocks separating the phosphate layers from area of Kouribgua (Morocco)[12-13]. The remaining insoluble uranium (60%) was in the uranate form (UO₄)²⁻. The experimental procedure consisted in extracting apatite in solution of sodium hydroxide in the presence of Cetrimonium bromide as a structuring agent in order to improve the porosity of the final product.

After extraction of apatite, the obtained liquor is strongly basic and its' neutralization is very crucial. For this, we used an ammonium salt because it presented a dual advantage: produce Ammonia and minimize the negative impact on environment. In fact, the ammonia produced during neutralization of alkaline liquor can be valued and recovered in two ways. In the first way, Ammonia can be recycled into ammonium chloride by collecting the gas in a diluted

solution of hydrogen chloride. In the second way, it can be dissolved in water to be used for synthesis of compound nano-fertilizer (NP or NPK-type) from the obtained apatite gel. In the present work, we have limited ourselves to recovering the gas of ammonia by collecting it in water. The reactions involved in the process of neutralization of liquor with an ammonia salt and its' recycling are illustrated by equations (1) and (2) below:



3. RESULTS AND DISCUSSION

3.1 X-ray diffraction analysis

X-ray diffraction was used to identify the phases in the raw material and the apatite gel obtained by alkaline extraction process. The used diffractometer type was a BRUKER equipped with a LYNXEYE detector and a copper tube with a wavelength $\lambda = 1.542\text{\AA}$.

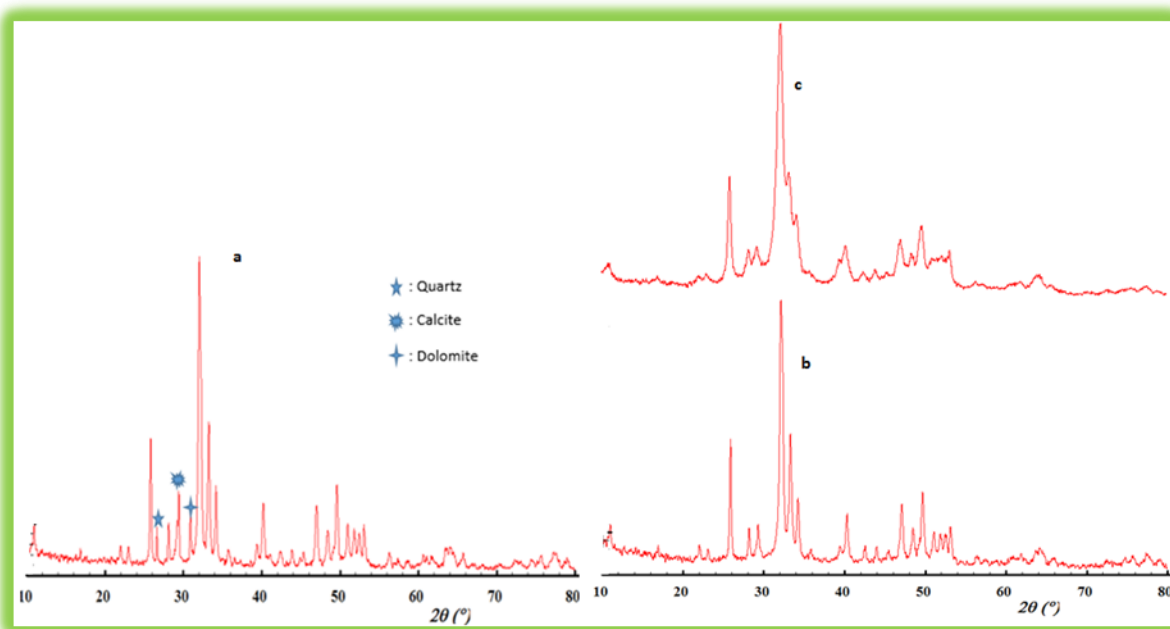


Figure 1: XRD spectrum of (a) crude phosphate sieved between 90 and 1000 μm , (b) apatite obtained by gelation in aqueous solution; (c) XRD Spectrum of apatite obtained by gelation in the presence of Cetrimonium bromide

The quantity of minerals associated with crude Apatite sieved between 90 and 1000 μm have become largely reduced, namely Quartz, calcite and dolomite (Fig. 1a). However, organic matter and amorphous silica cannot be detected by XRD.

The gels obtained by alkaline extraction process (fig. 1b & 1c) characterized the same single-phase structure corresponding to Hydroxyapatite ($\text{Ca}_{10}(\text{PO}_4)_6(\text{OH})_2$). There is a disappearance of

secondary phases that were identified in the raw material (Fig.1a). However, the diffraction lines corresponding to the gelation of apatite in pure aqueous solution are well resolved (Fig.1b). The gelation in presence of Cetrimonium bromide has led to a poorly crystallized apatite and therefore more reactive (Fig. 1c). We can conclude that the using of Cetrimonium bromide has allowed to produce the new additional surfaces of particles compared to those created in aqueous solution. This increases the specific area and improves reactivity and solubility. The solubility has increased by substitution of F^- by OH^- during conversion of fluorapatite into hydroxyapatite because the solubility product constant of fluorapatite is about one order of magnitude (12 times) smaller than that of hydroxyapatite [14].

3.2 FTIR analysis of functional groups

The main functional groups of the raw phosphate rock was identified with an infrared spectroscopy technique by using SCO-TECH spectrometer. The spectral studied range is between 400 cm^{-1} and 4000 cm^{-1} with resolution of 2 cm^{-1} . The measurements were conducted in absorbance through KBr pellets in which the powders to be analyzed are diluted. A mount of 1.5 mg of powder, previously crushed in an agate mortar, is intimately mixed with 300 mg of KBr. The pellet was formed by pressing this mixture with a pressure of 10 MPa. The results of this FTIR analysis were shown in Fig.2 below:

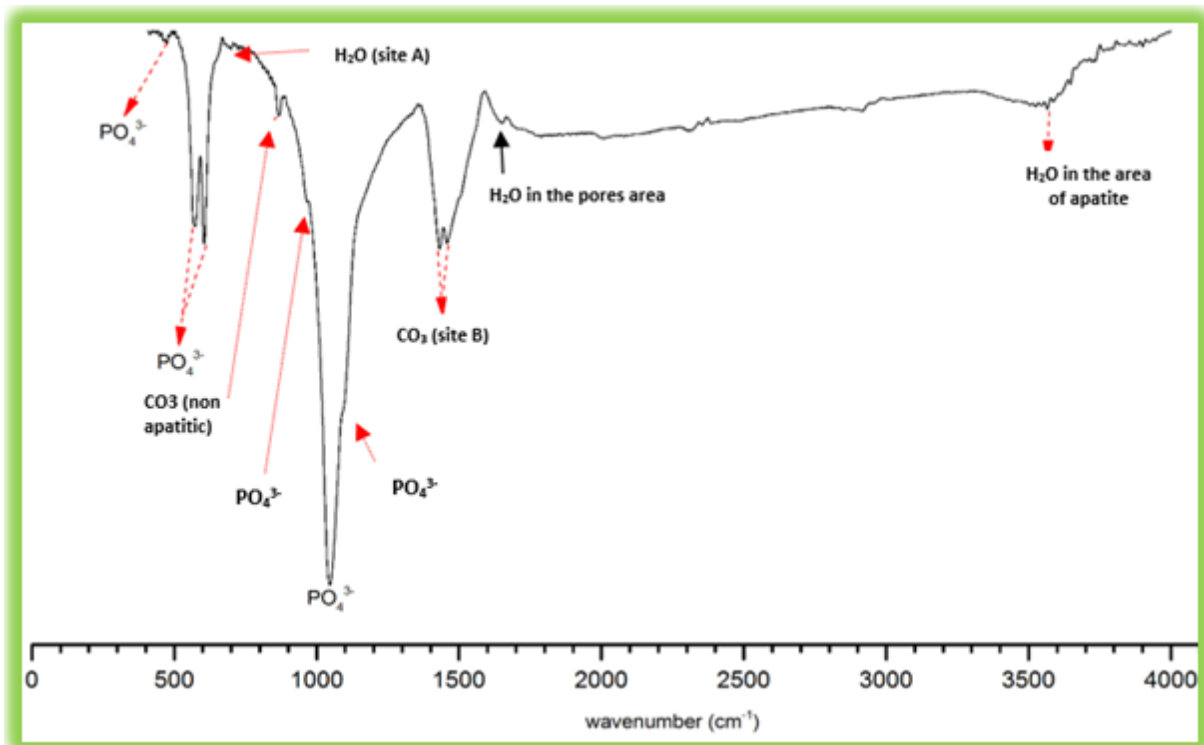


Figure2. Infrared spectrum of crud phosphate, sieved between 90 and 1000 μm

The spectrum of crude phosphate shows absorption bands characteristic of phosphate groups (PO_4^{3-}) at 1080, 1047, 960, 605, 569 and 473cm^{-1} respectively. The presence of a wide band at 3570cm^{-1} is attributable to stretching vibrations of OH^- bonds of water contained in the sample structure. The vibration bands observed at 1457 and 1423cm^{-1} correspond to the carbonate groups (CO_3^{2-}) incorporated in site B of apatite structure [15]. The band of vibration appearing at 870cm^{-1} corresponds to non apatitic carbonates (CO_3^{2-}) (dolomite + calcite) [16]; and this is in agreement with the results obtained by X-ray diffraction. The presence of a small absorption band at 680cm^{-1} correspond to the hydroxyl ions (OH^-) of water (site A of apatite) [17]. Finally, the small vibration band appearing at 1648cm^{-1} is attributable to the trapped water molecules in the pores by capillarity [18]. At the mineralogical level, we can say that the apatite of Bengerir has the characteristics of a carbonated fluorapatite with the chemical formula $\text{Ca}_{10}(\text{PO}_4, \text{CO}_3)_6(\text{F}_2, x\text{H}_2\text{O})$.

The analysis of functional groups present in the apatite obtained by alkaline extraction was carried out on the non-calcined and calcined gels for comparative purposes. The results obtained are shown in Fig. 3 below:

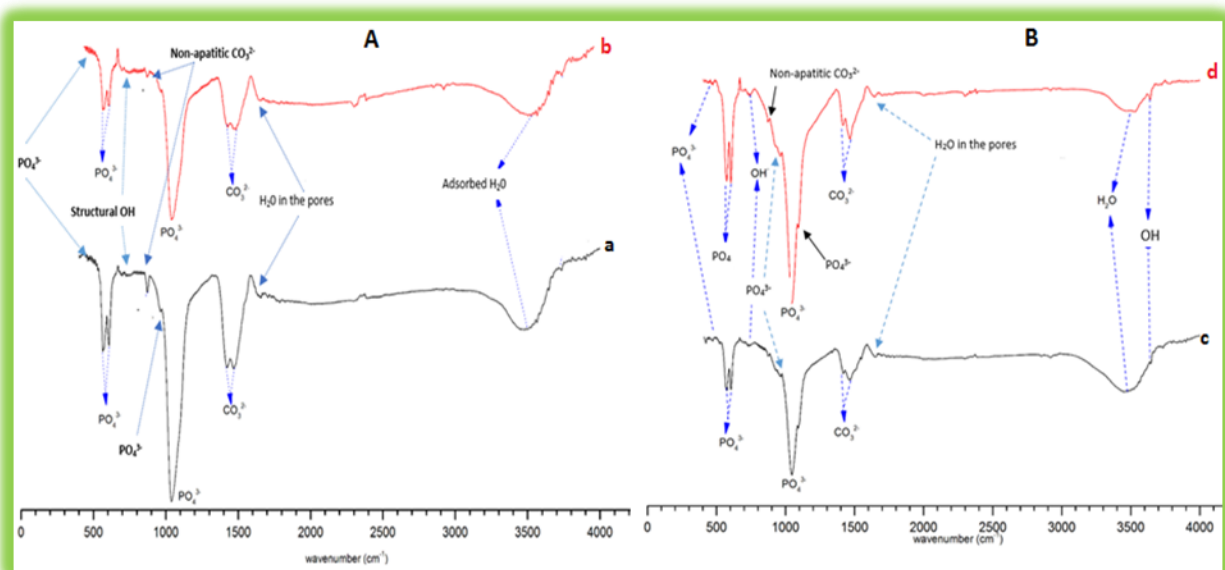


Figure 3: (A) FTIR of non calcined HAp where **a** was no treated by Cetrimonium and **b** was treated with Cetrimonium; (B) FTIR for HAp calcined at 800°C where **c** was no treated by Cetrimonium and **d** was treated with Cetrimonium bromide

The IR spectra show the appearance of a new vibration band at 635cm^{-1} corresponding to the structural groups (OH^-) [19]. This proves that the alkaline extraction process has allowed us to transform the fluorapatitic form of natural phosphate into hydroxyapatite. In addition, we note that the majority of vibration bands (PO_4^{3-}) that were observed in raw phosphate were found including carbonates (CO_3^{2-}).

However, it can be seen that calcination at 800°C did not remove non apatitic carbonate ions, even those located in the site B of apatite (1457 and 1431cm⁻¹). On the other hand, the vibration band located at 635cm⁻¹, which characterizes the structural ions (OH)⁻, has its intensity increased in the HAp calcined at 800°C (Fig.3B). In addition, as well as the bands corresponding to the carbonates located in site B of the apatitic structure, we notice a very clear resolution of bands corresponding to the groups (PO₄)³⁻. These results sufficiently proved that the process developed makes it possible to produce high proportion of Apatite and to preserve the apatitic structure of phosphate.

3.3 Porosity measurement

In this study, the measurement of porosity with BET method was made because the quality of XRD-spectra is not sufficient to estimate the pore size of crystallites, even though the width of peaks indicates that the obtained gels are probably nanometric. However, the strong point of XRD is the ease with which we can have access to the crystallite size, using the below relationship of Laue scherrer[20]: $S_c = \frac{0.9\lambda}{FWHM * \cos\theta}$ (1)

S_c is the average crystallite size (nm); λ is the wavelength of X-ray radiation (1.5406 Å); FWHM is the full width at half maximum for the diffraction peak under consideration (rad); and θ (degree) is the diffraction angle of the investigated peak. The type of peak concerned by measurement of FWHM is 00l, in particular the line 002 whose its angular position is 25.8° in 2θ as shown in the fig.4 below:

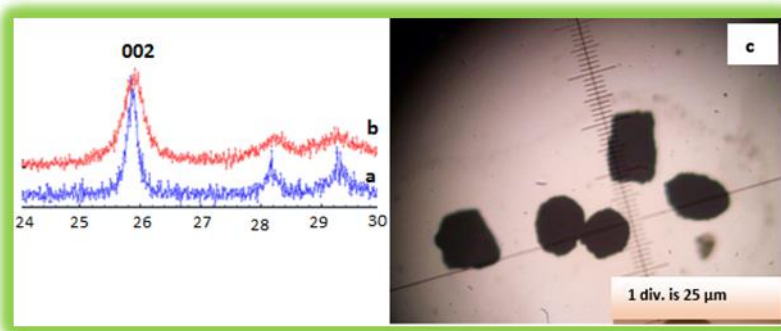


Figure4:XRD spectrum of apatitic gel (a)treated without Cetrimoniumwhere FWHM = 0.1153°, (b) treated with Cetrimoniumwhere FWHM = 0.6521°, (c) rounded and prismatic shape for crystals of natural phosphate observed by the optical microscope

The shape constant of the crystallites can be calculated from Bayer's relationship (2) valid for sizes less than one tenth of a micrometer: $Cst = \varnothing_c * S_{BET} * \rho_{Th}$ (2);

Where \varnothing_c , S_{BET} and ρ_{Th} are expressed in nm, m²/g and g/cm³. ρ_{Th} (HAp) = 3.156g/cm³ according to the literature [21].Cst = 2-3 for platelet morphology; Cst = 5-6 for rounded to spherical morphology; Cst = 3-5 for other composed morphology.

The specific area of our samples were measured by a physisorption device (Analyzer-Micromeritics 3FLEX), measuring the quantity of N₂ adsorbed as a function of pressure. The experiment was conducted at temperature of N₂ liquid-vapor equilibrium (77k). Before analysis, degassing of powders was carried out by heating at 250°C under reduced pressure (50-100mbar) for 12 hours. BET measurements were conducted on the non-calcined samples because the increase in temperature during the treatment of powder activates the growth of particles and causes a decrease in specific area [22].

The sorption isotherms obtained from the two HAp gels (fig. 5) are type IV, which are characteristic of a mesoporous material in accordance with the BET isothermal equation. Indeed, mesoporous materials are characterized by Hysteresis loops, which have a type IV character [23]

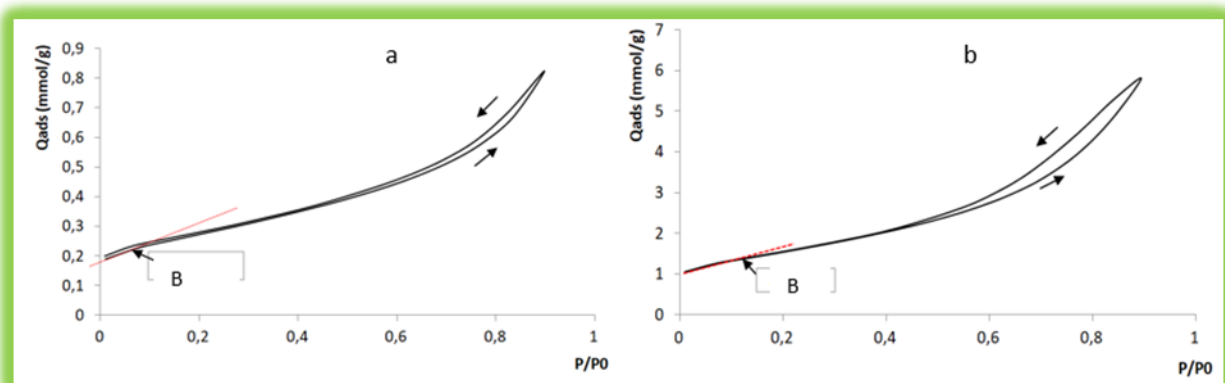


Figure .5: Type IV isotherms characterizing mesoporous materials: (a) HAp non treated with Cetrinonium, (b) HAp treated by Cetrinonium bromide

It is known that the closing of these hysteresis loops never ends with a plat and the desorption curve is more difficult to plot its limits (Fig.6a). It can be seen that point B characterizing the monolayer cover is related to the monolayer thickness Q_{ads}^{mono} (Fig.6). This point B corresponds to the first point of slope change.

The calculation of specific area S_{BET} for HAp is obtained by using the relationship (3):

$$S_{BET} = 4.38 \times V_{ads}^{mono} \quad (3) ; \quad \text{where} \quad V_{ads}^{mono} = 22.414 \times Q_{ads}^{mono}$$

The calculation of the size of mesopores is deduced from Kelvin's equation (4):

$$r_K(\text{nm}) = \frac{-0.96}{\ln P/P_0} \quad (4)$$

Where r_K is the Kelvin radius corresponding to the radius of the meniscus produced either in a pore of radius r_K if pore has a cylindrical form. In this case, $r_K = r_p - t$, where t is the thickness of the multilayer adsorbed at relative pressure (P/P₀).

The plotting of the curve Q as a function of t from Harkin' equation (5) gives a line (Fig.6):

$$\ln(P_0/P) = 2A_m^f / t^2 \quad (5)$$

The deviation from linearity represents the point of the multilayer capacity noted PCMult allowing access to the porous volume V_p by using the Gurvich's rule (6):

$$V_l(N_2) = V_p = \frac{m_{ads}^{mult}}{\rho(N_2)} \quad (6);$$

Where $A_m^f (\text{\AA}^2)$ is the mass area of the molecular fluid used (12.5\AA^2 for N_2 molecule which is in strong interaction with the surface of the adsorbent; 16.2\AA^2 if the N_2 molecule is in weak interaction with the surface of adsorbent); where $m_{ads}^{mult} = Q_{ads}^{mult} \times M_{N_2}$; $\rho(N_2) = 0.808 \text{ g/cm}^3$

However, Kelvin's equation is only strictly exact if the pore size is greater than 7.5 nm [24]. If the value is smaller than this size, the deviation from the real value can be 30% lower for narrow mesopores ($2\text{nm} < \varnothing < 5 \text{ nm}$).

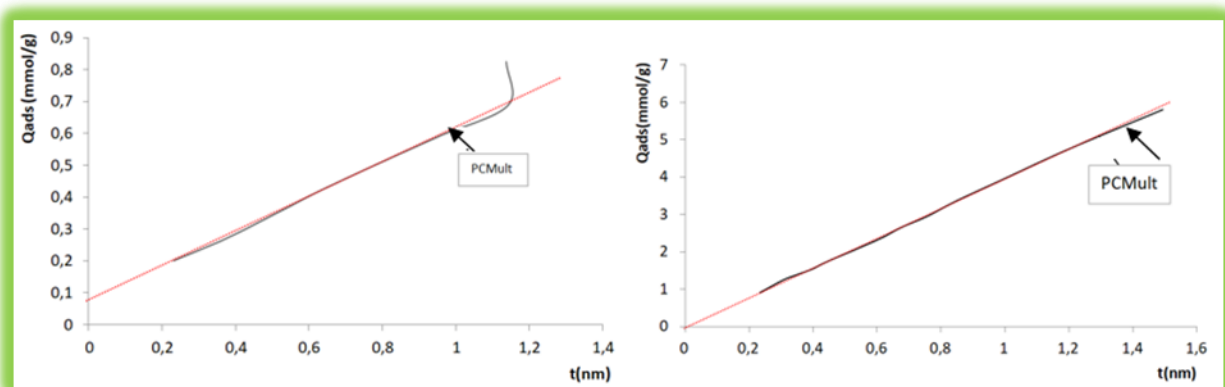


Figure 6: Transformed curve t in desorption mode of Hap: (a) Hap non-treated by Cetrimonium (b) Hap treated by Cetrimonium bromide

We obtain here a straight line passing rigorously through the origin, whose slope allows an access to the equivalent specific surface BET: $S_{BET} = \text{slope (mol/ g m)} \times V_m^{N_2}$ ($34.7 \text{ m}^3/\text{mol}$ for nitrogen).

The use of Harkin's equation for tracing the transformed curves $Q f(t)$ is applicable even for relative pressures P/P_0 which tend towards unity, unlike the BET equation which is only available in a restricted relative pressure range ($P/P_0 \leq 0.35$).

Table 1: Results of BET and XRD for apatite gels obtained in the absence and presence of Cetrimonium bromide

Apatite gel	ϕ_c (nm)	$S_{BET} = S_p + S_p V_{Pt}$ (m^2/g)	V_{Pt} (cm^3/g)	\varnothing_p (nm)	$*S_p$ (m^2/g)	$**\rho_a$ (g/cm^3)	Porosit y $1 - \rho_a / \rho_{th}$	Shape Cst
Non-treated by	70.7	21.6	0.020	8.0	10.4	~ 3	~ 5%	4.8

Cetrimonium			8					
Treated by Cetrimonium	12.5	137.4	0.187 1	16.8	44.5	~ 2	~ 37 %	5.4

* Value deduced from the relationship $S_p = \frac{4 \times V_p}{\phi_p}$

** Value deduced from the relationship $V_p = \rho_a^{-1} - \rho_{th}^{-1}$ with;
 $\rho_{th}(\text{HAp standard}) = 3.156 \text{ g/cm}^3$

The results of BET have shown that the gel obtained in the presence of Cetrimonium bromide has a surface area of six times greater than that of the gel obtained in aqueous medium (Table1). It can be seen that Cetrimonium bromide has the effect of strongly dispersing the aggregate HAp, which is manifested by a decrease in the size of the crystallites as well as an increase in the specific surface area while respecting Baver's relationship (2). In addition, the composed morphology of untreated HAp becomes spherical when HAp is treated with Cetrimonium bromide (Table 1 column 9). It is known that the specific BET surface area is a contribution of pore and particle surfaces: $S_{BET} = S_p + S_{part}$. Therefore, HAp treated with Cetrimonium bromide is expected to develop larger active surfaces than those developed by untreated HAp (Table 1 columns 3 and 6). However, the contribution of pores and particles is the same for untreated HAp (on average 50% : 50%). Concerning the HAp treated with Cetrimonium bromide, the contribution of pores and particles is in a proportion of 30%: 70%. It can therefore be concluded that structuring agents such as Cetrimonium bromide promote the formation of new active surfaces such as acid-base sites and have only a limited role on pores size.

4. CONCLUSION

The results of this study showed that our raw material sample was a carbonated fluorapatite. The alkaline extraction method has allowed us to manufacture a nano-porous fertilizer having a hydroxyapatitic structure. This material can constitute an important intermediate for synthesis of other phosphate derivatives such as compound nano-fertilizers and the possibility to produce a food-grade phosphoric acid. The synthesis of nano-porous Hydroxyapatite was made without any loss of materials contrary to the conventional process of acid attack which is accompanied by the production of huge amounts of waste in phosphogypsum form. According to some authors, the production of each ton of H_3PO_4 leads to a residue weighing about 5 tons of phosphogypsum depending on the quality of phosphate rocks[25].The simultaneous treatment of liquid waste and recycling of the used products has allowed us to make the process compatible with environment. The obtained hydroxyapatite at nanoscale and directly from phosphate rock has allowed us to contribute to eco-sustainability because 1kg of phosphate nano is equivalent to 1 ton of phosphate used as it is or at macrometric scale. This process therefore constitutes one of most promising routes for manufacture of pure apatite on an industrial scale from crude phosphate ore because it makes it possible to manufacture phosphate with very high benefit.

REFERENCES

- [1] Dawson, C. J., J. Hilton, (2011). Fertilizer availability in a resource-limited world: production and recycling of nitrogen and phosphorus, *Food Pol.*, vol. 36, pp. S14–S22.
- [2] Ibrahim, S. S., A. A. El-Midany, T. R. Boulos, Effect of intensive mechanical stresses on phosphate chemistry as a way to increase its solubility for fertilizer application *Physicochem. Probl. Miner. Process.*, vol. 44, pp 79-92, 2010.
- [3] Liu, R., and R. Lal. 2014. Synthetic apatite nanoparticles as a phosphorus fertilizer for soybean (*Glycine max*). *Scientific Reports* 4:5686. doi: 10.1038/srep05686.
- [4] Qureshi, A., D.K. Sing and S. Dwivedi, (2018). Nanofertilizers: A Novel Way for Enhancing Nutrient Use Efficiency and Crop Productivity. *Int. J. Curr. Microbiolo. App. Sci.* 7: 3325-3335.
- [5] Duhan, J.S., R. Kumar, N. Kumar, P. Kaur, K. Nehra, S. Duhan, (2017). Nanotechnology: The new perspective in precision agriculture. *Biotechnol. Rep.*15: 11-23.
- [6] Nair, R., S.H. Varghese, B.G. Nair, T. Maekawa, Y. Yoshida and D.S Kumar. 2010. Nanoparticulate material delivery to plants. *Plant. Sci.* 179: 154-163.
- [7] Pileni, M.P, (1997). Nanosized Particles Made in Colloidal Assemblies. *Langmuir.* 13: 3266-3276.
- [8] Moon, S.Y., T. Kusunose and T. Sekino. 2009. CTAB-Assisted Synthesis of Size- and Shape-Controlled Gold Nanoparticles in SDS Aqueous Solution. *Mater. Lett.*63: 2038-2040.
- [9] Wang, J., S.P. Huang, K. Hu, K.C. Zhou and H. Sun, (2015). Effect of cetyltrimethylammonium bromide on morphology and porous structure of mesoporous hydroxyapatite. *Trans. Nonferrous Met. Soc. China (English Edition).* 25: 483-489.
- [10] Arami, H., M. Mohajerani, M. Mazlumi, R. Khalifehzadeh, A. Lak and S. K. Sadrnezhad.(2009). Rapid formation of hydroxyapatite nanostrips via microwave irradiation. *J. Alloys Compd.* 469: 391-394.
- [11] Song, J., Y. Liu, Y. Zhang and L. Jiao, (2011). Mechanical properties of hydroxyapatite ceramics sintered from powders with different morphologies. *Mater. Sci. Eng. A.*528: 5421-5427.
- [12] Abbassi, Z. E., S. Belcadi, J.J. Rameau, (1986). Etude du comportement électrochimique des ions du Vanadium dans des mélanges eau-acide phosphorique, *Electrochimica Acta*, vol.31(11): 1467-1472.
- [13] Arambourg. C et J. Orcel .C. r. Acad. Sci., France, série C, 233, 1635 (1951).

- [14] Chow, L.C. and M. Markovic,(1998). Physicochemical Properties of Fluorapatite. In: Z. Amjad (ed.), Calcium Phosphates in Biological and Industrial Systems. Springer, Boston, MA. pp 67-83.
- [15] Fleet, M.E., X. Liu,(2007). Coupled substitution of type A and B carbonate in sodium-bearing apatite. *Biomater.*28: 916-926.
- [16] Birken, I., M. Bertucci, J. Chappelin and E. Jorda, (2016). Quantification of Impurities, Including Carbonates Speciation for Phosphates Beneficiation by Flotation. *Procedia Eng.*138: 72-84.
- [17] El Hammari, L., H. Merroun, T. Coradin, S. Cassaignon, A. Laghzizil and A. Saoiabi, (2007). Mesoporous hydroxyapatites prepared in ethanol-water media: Structure and surface properties. *Mater. Chem. Phys.*104: 448-453.
- [18] Amutha, K., R. Ravibaskar, G. Sivakumar, (2010). Synthesis and characterization of nanosilica from Rice Husk Ash, *.Int. J. Nanotech Appl.* 4: 61-66.
- [19] Panda, R. N., M.F. Hsieh, R.J. Chung, T.S. Chin, (2003). FTIR, XRD, SEM and solid state NMR investigations of carbonate-containing hydroxyapatite nano-particles synthesized by hydroxide-gel technique, *Journal of Physics and Chemistry of Solids* 64: 193–199.
- [20] Wu, S. C., H.K.Tsou, H.C.Hsu, S. K. Hsu, S. P.Liou, W. F.Ho, (2013). A hydrothermal synthesis of eggshell and fruit waste extract to produce nanosized hydroxyapatite,*Cer.Int.*39(7):8183–8188.
- [21] Kamalanathan, P., S. Ramesh, L.T. Bang, A. Niakan, C.Y. Tan, J. Purbolaksono and W.D. Teng, (2014). Synthesis and sintering of hydroxyapatite derived from eggshells as a calcium precursor. *Ceram. Int.*40: 16349-16359.
- [22] El Hammari, L., A. Laghzizil, P. Barboux, A. Saoiabi and K. Lahlil, (2004). Crystallinity and fluorine substitution effects on the proton conductivity of porous hydroxyapatites. *J. Solid State Chem.*177: 134-138.
- [23] Brunauer, S., P. H. Emmett and E. Teller, (1938). Adsorption of Gases in Multimolecular Layers. *J. Am. Chem. Soc.*60: 309-319.
- [24] Rouquerol, J., F. Rouquerol, K. S. W. Sing, P. Llewellyn, G. Maurin. *Adsorption by Powders and Porous Solids: Principles, Methodology and Applications*, Academic Press (2014).
- [25] Far Felfoul H., P. Clastres, M. Ben ouezdou, A. Carles-Gibergues,(2002). Properties and perspectives of valorization of phosphogypsum the example of Tunisia, *EPCOWM'2002*: 510-520